Contribution from the Science Research Laboratory, 3M Central Research Laboratory, St. Paul, Minnesota 55101, and the Department of Chemistry, University of Minnesota, Minneapolis, Minnesota 55455

Structure of Palladium Bis(hexafluoroacetylacetonate) and the Systematics of Its Acid–Base Chemistry

A. R. SIEDLE,*[1a] R. A. NEWMARK,[1a] and L. H. PIGNOLET*[1b]

Received September 16, 1982

Palladium bis(hexafluoroacetylacetonate), $Pd(F_6acac)_2$, crystallizes from the vapor in space group $P\bar{1}$, triclinic, with $a = 12.279$ (4) Å, $b = 12.815$ (2) Å, $c = 4.894$ (2) Å, $\alpha = 93.63$ (3)°, $\beta = 91.81$ (3)°, $\gamma = 89.51$ (2)°, and $Z = 2$. The structure solution, obtained from 2073 reflections, converged at $R = 0.063$ and $R_w = 0.084$. It is essentially a molecular crystal with two unique half-molecules, each lying on an inversion center, per unit cell. The F_6acac ligands are planar with $d(\text{Pd–O})_{av} = 1.967$ (5) Å. The two metal atoms are displaced from their chelate planes by 0.008 and 0.039 Å. X-ray crystallographic studies of $Pd(F_6acac)_2L_n$ have identified three bonding types for the F_6acac ligands. They are η^2 oxygen bonded (F_6acac-*O,O'*), η^1 bonded through the central methine carbon (F_6acac-*C*), and η^1 oxygen bonded or semichelating (F_6acac-*O*). Here, the systematics of the solution-phase acid–base chemistry were probed by ^1H and ^{19}F NMR spectroscopy. This fluorinated metalloorganic is a strong Lewis acid and reacts with Lewis bases by sequential cleavage of the four Pd–O bonds. Interaction with 1 equiv of a donor, L, produces $Pd(F_6acac\text{-}C)(F_6acac\text{-}O,O')L$ and $Pd(F_6acac\text{-}O)(F_6acac\text{-}O,O')L$. Both are converted by additional base into $Pd(F_6acac\text{-}O,O')L_2{}^+F_6acac^-$. Additional base cleaves the remaining two Pd–O bonds to generate $Pd(F_6acac\text{-}O)L_3{}^+F_6acac^-$ and then $PdL_4{}^{2+}(F_6acac^-)_2$.

Introduction

Palladium bis(hexafluoroacetylacetonate), $Pd(F_6acac)_2$, is, on account of the electron-withdrawing effect of the four trifluoromethyl groups, a strong Lewis acid. Although it exhibits pronounced acceptor behavior toward ligands containing nitrogen, sulfur, selenium, phosphorus, and arsenic, it has a low affinity for oxygen donors and is isolated in anhydrous form from aqueous media. In contrast, $Ni(F_6acac)_2$ is obtained as an octahedral dihydrate in which only the axial water molecules are appreciably labile.[2a] Similarly, copper(II) and zinc hexafluoroacetylacetonates react with pyridine to form the six-coordinate bisadducts $M(F_6acac)_2(C_5H_5N)_2$.[2b,3] The reluctance of palladium to expand its coordination sphere in $Pd(F_6acac)_2$ by accepting axial ligands contributes significantly to reactions of this fluorinated metalloorganic that proceed by displacement mechanisms. Thus, the acid–base chemistry of $Pd(F_6acac)_2$ is quite broad in scope. Complexes of the type $Pd(F_6acac)_2L_n$ (L = ligand; n = 1–4) have been characterized for a wide variety of molecular donors,[4-8] and those of the n = 2 class have been reported for the condensed-phase donors alumina[9] and silica.[10] Acid–base complexes have been recognized as intermediates in ortho-metalation reactions of $Pd(F_6acac)_2$[11] and are probably involved in synthetic reactions that lead to bis(formazanyl)palladium compounds[12] and the dimeric alkoxide $Pd_2(\mu\text{-}CH_3O)_2(F_6acac)_2$.[13] In this paper, we report the crystal and molecular structure of the parent $Pd(F_6acac)_2$ and a detailed NMR investigation that outlines the systematics of its rather complex reactions with Lewis bases.

Table I. Positional Parameters

atom	*x*	*y*	*z*
Pd1	0.0000 (0)	0.0000 (0)	0.0000 (0)
Pd2	0.5000 (0)	0.5000 (0)	0.5000 (0)
F1	0.2944 (7)	−0.0145 (9)	0.618 (2)
F2	0.3488 (6)	0.0661 (11)	0.310 (2)
F3	0.3015 (7)	0.1331 (9)	0.702 (2)
F4	−0.0303 (8)	0.3011 (7)	0.763 (2)
F5	−0.0987 (9)	0.3301 (6)	0.379 (2)
F6	−0.1689 (7)	0.2231 (7)	0.610 (2)
F7	0.2250 (8)	0.3388 (7)	−0.007 (3)
F8	0.1320 (8)	0.4428 (13)	0.235 (3)
F9	0.1519 (8)	0.4735 (9)	−0.132 (2)
F10	0.5164 (8)	0.7646 (7)	−0.094 (2)
F11	0.4278 (11)	0.8256 (6)	0.197 (2)
F12	0.3655 (9)	0.7645 (7)	−0.195 (2)
O1	0.1440 (5)	0.0107 (5)	0.196 (1)
O2	0.3638 (5)	0.4424 (5)	0.335 (1)
O3	0.4943 (5)	0.6274 (5)	0.298 (1)
O4	−0.0628 (5)	0.1175 (5)	0.217 (1)
C1	0.1651 (8)	0.0761 (8)	0.378 (2)
C2	0.0935 (8)	0.1591 (8)	0.503 (2)
C3	−0.0098 (8)	0.1699 (7)	0.408 (2)
C4	0.2823 (9)	0.0704 (10)	0.495 (3)
C5	−0.0744 (10)	0.2578 (10)	0.538 (2)
C6	0.3099 (8)	0.4921 (8)	0.155 (2)
C7	0.3274 (9)	0.5859 (8)	0.060 (2)
C8	0.4165 (8)	0.6488 (8)	0.138 (2)
C9	0.2070 (9)	0.4292 (9)	0.050 (3)
C10	0.4263 (9)	0.7550 (8)	0.015 (3)
H2	0.1208 (0)	0.2069 (0)	0.6504 (0)
H7	0.2732 (0)	0.6106 (0)	−0.0697 (0)

Results

Structure of Palladium Bis(hexafluoroacetylacetonate). Solid $Pd(F_6acac)_2$ comprises essentially a molecular crystal. There appears to be no significant intermolecular contacts, and the shortest intermolecular Pd–Pd distance is 4.89 Å, precluding any strong metal–metal bonding. This Pd–Pd separation represents a unit translation along the *c* crystallographic axis. There are two crystallographically unique half-molecules in the unit cell, each lying on an inversion center. Figure 1 shows ORTEP drawings and labeling schemes for each molecule. Atomic coordinates and selected bond

---

(1) (a) 3M Central Research Laboratory. (b) University of Minnesota.

(2) (a) R. L. Pecsok, W. D. Reynolds, J. P. Fackler, Jr., I. Lin, and J. Pradilla-Sorzano, *Inorg. Synth.*, **15**, 96 (1974). (b) J. Pradilla-Sorzano and J. P. Fackler, Jr., *Inorg. Chem.*, **12**, 1174 (1973).

(3) J. Pradilla-Sorzano and J. F. Fackler, Jr., *Inorg. Chem.*, **12**, 1182 (1973).

(4) A. R. Siedle and L. H. Pignolet, *Inorg. Chem.*, **20**, 1849 (1981).

(5) A. R. Siedle, R. A. Newmark, A. A. Kruger, and L. H. Pignolet, *Inorg. Chem.*, **20**, 3399 (1981).

(6) A. R. Siedle, R. A. Newmark, and L. H. Pignolet, *J. Am. Chem. Soc.*, **103**, 4947 (1981).

(7) A. R. Siedle and L. H. Pignolet, *Inorg. Chem.*, **21**, 135 (1982).

(8) A. R. Siedle, R. A. Newmark, and L. H. Pignolet, *J. Am. Chem. Soc.*, **104**, 6584 (1982).

(9) A. R. Siedle, P. M. Sperl, and T. W. Rusch, *Appl. Surf. Sci.*, **6**, 149 (1980).

(10) A. R. Siedle and R. A. Newmark, *J. Am. Chem. Soc.*, **103**, 1240 (1981).

(11) A. R. Siedle, *J. Organomet. Chem.*, **208**, 115 (1981).

(12) A. R. Siedle and L. H. Pignolet, *Inorg. Chem.*, **19**, 2052 (1980).

(13) A. R. Siedle and L. H. Pignolet, *Inorg. Chem.*, **21**, 135 (1982).

0020-1669/83/1322-2281$01.50/0 © 1983 American Chemical Society

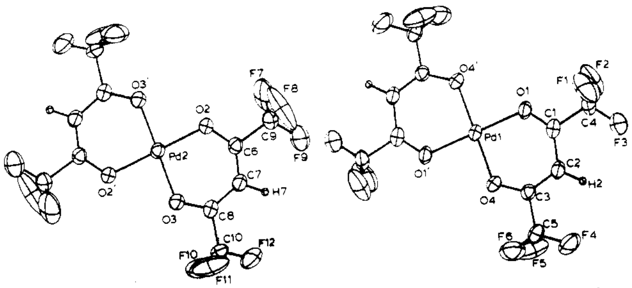

Figure 1. ORTEP drawing of the two independent molecules of Pd(F_6acac)$_2$ showing 30% probability ellipsoids. Both molecules have inversion centers at the Pd atoms.

Table II. Selected Distances and Angles in Pd(F_6acac)$_2$

	Distances, Å		
Pd1–O1	1.987 (5)	Pd2–O2	1.963 (5)
Pd1–O4	1.955 (5)	Pd2–O3	1.961 (5)
O1–C1	1.21 (1)	O2–C6	1.28 (1)
O4–C3	1.279 (9)	O3–C8	1.256 (9)
C1–C2	1.49 (1)	C6–C7	1.34 (1)
C2–C3	1.35 (1)	C7–C8	1.39 (1)
C3–C5	1.49 (1)	C8–C10	1.53 (1)
	Angles, deg		
O1–Pd1–O4	93.7 (2)	O2–Pd2–O3	94.9 (2)
O1–Pd1–O4	86.3 (2)	O2–Pd2–O3	85.1 (2)
Pd1–O1–C1	123.5 (5)	Pd2–O2–C6	120.3 (5)
Pd1–O4–C3	123.3 (5)	Pd2–O3–C8	123.1 (5)
O1–C1–C2	129 (1)	O2–C6–C7	130 (1)
O4–C3–C2	130 (1)	O3–C8–C7	127 (1)
C1–C2–C3	120 (1)	C6–C7–C8	124 (1)
O1–C1–C4	114 (1)	O2–C6–C9	111 (1)
C2–C1–C4	117 (1)	C7–C6–C9	119 (1)
O4–C3–C5	113 (1)	O3–C8–C10	114 (1)
C2–C3–C5	117 (1)	C7–C8–C10	119 (1)

distances and angles are given in Tables I and II.

There are some significant differences between chemically equivalent distances and angles within the two molecules, the most notable of these being the unusually short C1–O1 distance (1.21 (1) Å) compared to the average of the other three C–O distances (1.27 (1) Å) and the unusually long C1–C2 distance (1.49 (1) Å) compared to the average of the other three F_6acac chelate-ring C–C distances (1.36 (1) Å). We suggest that these differences are due to crystal-packing forces or to disorder (vide infra) in the C4 CF_3 group since there is no obvious reason that portions of chemically equivalent molecules should be so different. Most of the chemically equivalent distances and angles in the two molecules are the same within experimental error.

Each Pd(F_6acac)$_2$ molecule contains two bidentate, chelating F_6acac ligands. The distances and angles within the planar

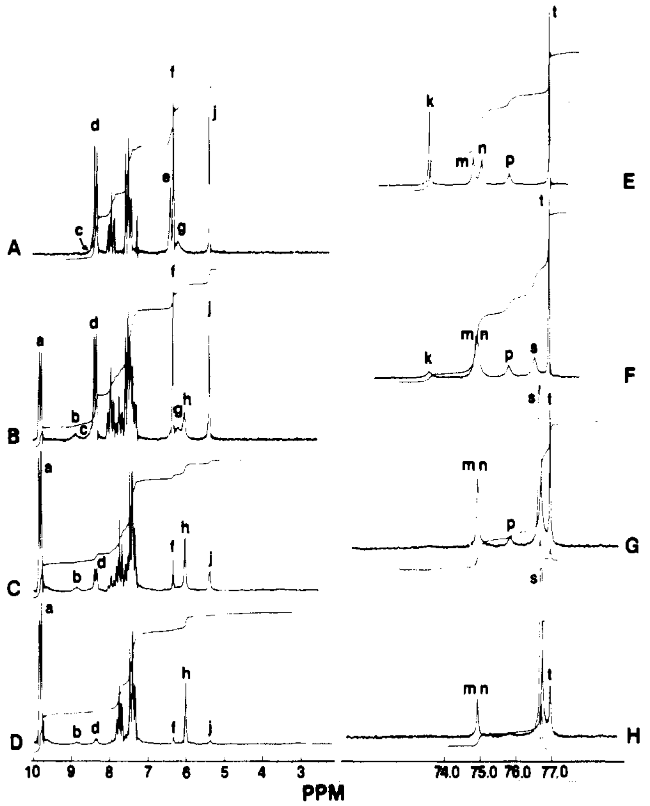

Figure 2. ^{1}H and ^{19}F NMR spectra of pyridine–Pd(F_6acac)$_2$ mixtures. ^{1}H NMR, py:Pd(F_6acac)$_2$: (A) 0.5:1; (B) 1.4:1; (C) 2.7:1; (D) 3.8:1. ^{19}F NMR, py:Pd(F_6acac)$_2$: (E) 0.5:1; (F) 1.4:1; (G) 2.7:1; (H) 3.8:1.

chelate rings are normal except as noted above. The F_6acac ligands are planar with maximum displacements from the O1, O4, C1, C2, C3 and O2, O3, C6, C7, C8 least-squares planes of 0.008 and 0.039 Å, respectively. The Pd atoms are displaced 0.006 and 0.019 Å, respectively, from these planes (see supplementary material). The O–Pd–O angles are similar for the two molecules and have average values of 94.3 (2) and 85.7 (2)° for the chelate and nonchelate angles, respectively. Therefore, the molecules are essentially square planar. The average Pd–O distance of 1.967 (5) Å is significantly shorter than those in the Pd(F_6acac)$_2$ complexes Pd(F_6acac)$_2$·Me_2NH (d(Pd–O)$_{av}$ = 2.03 Å)[5] and [(bpy)Pd(F_6acac)]F_6acac (d(Pd–O)$_{av}$ = 2.005 Å)[6] but, despite the greater reactivity of Pd(F_6acac)$_2$ toward nucleophiles, is similar to that in the nonfluorinated analogue Pd(acac)$_2$ (d(Pd–O)$_{av}$ = 1.979 Å) in its crystal complex with tetrathiafulvalene[14] and to d(Pd–O)$_{av}$ =

Table III. Spectroscopic Data for Pd(F_6acac)$_2$ Complexes

	LPd(F_6acac-*C*)(F_6acac-*O,O'*)			LPd(F_6acac-*O*)-(F_6acac-*O,O'*)		[L_2Pd(F_6acac-*O,O'*)]$^+$-F_6acac$^-$		$(L_4Pd)^{2+}$(F_6acac$^-$)$_2$	
ligand (L)	δ(^{1}H)	δ(^{19}F)	ν(CO)[a]	δ(^{1}H)	δ(^{19}F)	δ(^{1}H)	δ(^{19}F)	δ(^{1}H)	δ(^{19}F)
Ph_3As	4.60 6.22	75.64 75.71 76.23	1745	5.9	76.39	5.91	75.97		
C_5H_5N	5.40 6.34	74.94 75.11 76.99	1738	6.2	75.86			6.02	76.71
i-$PrNH_2$	5.21 6.30	75.13 75.28 77.45	1724	6.3	75.03			5.95	77.65
1,4-$C_4H_8S_2$	5.08 6.13	74.44 76.64	1735			5.54	76.35		
t-BuNC	5.10 6.32	75.05 75.29 77.56	1747						

[a] cm^{-1}.

Table IV. Ratios of $Pd(F_6acac)_2$ and $L_nPd(F_6acac)_2$ Species as a Function of Ligand Concentration

		rel concn, %				
ligand (L)	ratio of L:Pd	Pd-$(F_6acac)_2$	LPd-(F_6acac-*O,O'*)-(F_6acac-*C*)	LPd-(F_6acac-*O,O'*)-(F_6acac-*O*)	L_2Pd-$(F_6acac)_2$	L_4Pd-$(F_6acac)_2$
py	0.47:1	53	43	6		
	0.74:1	26	63	11		
	1.35:1	5	67	10	6	12
	2.70:1	1	39	5	5	50
	3.80:1	0	17	2	4	78
Ph_3As	0.54:1	56	14	28	2	...
	1.07:1	9	26	56	8	...
	2.00:1	0	0	0	100	0
i-$PrNH_2$	0.88:1	28	53	9	9	2
	1.24:1	15	53	17	3	12
dithiane	0.51:1	34	18	48[a]		
	0.93:1	16	7	77[a]		
	2.40:1	0	0	100[a]		
t-BuNC	1.11:1	2	84	14[a]		

[a] Includes other species in rapid equilibrium.

1.975 (5) Å in *cis*-bis(1-phenyl-1,3-butanedionato)palladium.[15]

Sequential Displacement Reactions. The reaction of pyridine with $Pd(F_6acac)_2$ provides much insight into the general systematics of $Pd(F_6acac)_2$ acid–base chemistry. This system was studied in chloroform solution by ^1H and ^{19}F NMR spectroscopy using different amine:Pd ratios. Typical spectra are shown in Figure 2, and spectroscopic data for the compounds observed are collected in Table III.

As the pyridine:$Pd(F_6acac)_2$ ratio increases, resonances e and k ($\delta(^1H)$ 6.42 and $\delta(^{19}F)$ 73.64) due to free $Pd(F_6acac)_2$ disappear. Concomitantly, resonances due to two 1:1 adducts appear at low py:Pd ratio; cf. spectra A, B, E, and F in Figure 2. The molar ratios are given in Table IV. The 1:1 pyridine:$Pd(F_6acac)_2$ ratios are determined by integration, and their characteristic NMR peaks are greatly diminished when the pyridine:Pd ratio is ≥2:1 (spectra C and G). The 1:1 complex present in greater amount has F_6acac methine signals at 5.40 and 6.34 ppm in a 1:1 ratio (peaks j and f, respectively) and a pyridine α-proton doublet at 8.38 ppm (peak d). The proton integration proves the 1:1 complex contains two F_6acac methine protons per pyridine. The ^{19}F NMR spectrum of this material comprises singlets at 74.94, 75.11, and 76.99 ppm (peaks m, n, and t, respectively). These resonances occur in a 1:1:2 ratio, characteristic of 1:1 adducts containing a F_6acac ligand bonded to palladium through the methine carbon (F_6acac–*C*).[4] Therefore, this first complex is Pd(F_6acac-*O*,*O'*)(F_6acac-*C*)py. In agreement with this assignment, the infrared absorption at 1738 cm^{-1}, due to the uncoordinated carbonyl groups in the $Pd-CH(COCF_3)_2$ moiety, is proportional to the areas of ^{19}F peaks m, n, and t.

The second 1:1 adduct displays a broad methine C–H resonance at 6.2 ppm (peak g), a pyridine α-hydrogen peak at 8.42 ppm (peak c), and a CF_3 peak at 75.86 (peak p). Proton integration confirms the 1:1 ratio. These NMR data are quite similar to those for $Pd(F_6acac)_2PPh_3$, which has been shown by X-ray crystallography[8] to have attached to palladium one bidentate, oxygen-bonded F_6acac group (F_6acac-*O,O'*) and one monodentate, oxygen-bonded F_6acac diketonate ligand (F_6acac-*O*), which we have referred to as semichelating F_6acac.[6] We have previously established that phosphine adducts of the class Pd(F_6acac-*O,O'*)(F_6acac-*O*)P(aryl)$_3$ are stereochemically nonrigid and that the F_6acac-*O* and F_6acac-*O,O'* groups rapidly interconvert on the NMR time scale. We conclude, therefore, that the second 1:1 pyridine adduct is Pd(F_6acac-*O,O'*)(F_6acac-*O*)py and that a similar fluxional process leads to the observed averaged ^{19}F and methine proton resonances.

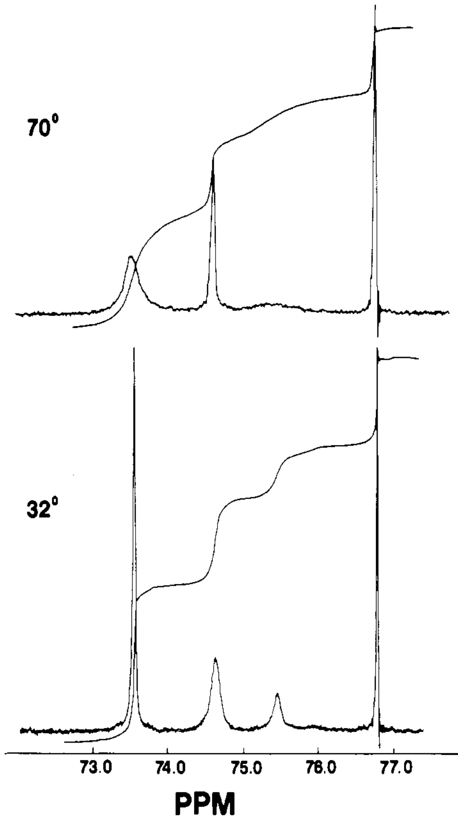

Figure 3. ^{19}F NMR spectra of 0.5:1 py:$Pd(F_6acac)_2$ in toluene at 32 and 70 °C.

The two isomeric 1:1 pyridine complexes appear not to rapidly interconvert. Figure 3 shows the ^{19}F NMR spectrum of a 0.5:1 mixture of pyridine and $Pd(F_6acac)_2$ in toluene. In addition to a peak due to free $Pd(F_6acac)_2$ at 75.36 ppm, resonances at 74.64 and 76.80 ppm, associated with Pd(F_6acac-*O,O*)(F_6acac-*C*)py, and at 75.47 ppm, due to Pd(F_6acac-*O,O'*)(F_6acac-*O*)py, are seen. With an increase of temperature from 32 to 70 °C, the latter isomer, containing the semichelating F_6acac, exchanges pyridine with $Pd(F_6acac)_2$ as both the 75.36- and 75.47-ppm signals broaden from 3 to 21 Hz and from 11 to ca. 54 Hz, respectively, while peaks due to the carbon-bonded isomer sharpen slightly. The ratio of

---

(14) A. R. Siedle, T. J. Kistenmacher, R. M. Metzger, C. S. Kuo, R. P. VanDuyne, and T. Cape, *Inorg. Chem.*, **19**, 2048 (1980).

(15) S. Okeya, S. Ooi, K. Matsumoto, Y. Nakamura, and S. Kawaguchi, *Bull. Chem. Soc. Jpn.*, **54**, 1085 (1981).

$Pd(F_6acac\text{-}O,O')(F_6acac\text{-}C)py$ to $Pd(F_6acac\text{-}O,O')(F_6acac\text{-}O)py$ is solvent dependent. In this experiment, using toluene solvent, it was 4.2:1 compared to 6.7:1 in chloroform.

Spectra B and F, in which the pyridine:$Pd(F_6acac)_2$ ratio is 1.4:1, are more complicated. In addition to the resonances of the two 1:1 complexes, those due to $[Pd(py)_4](F_6acac)_2$ are quite pronounced. This species exhibits a singlet ^{19}F peak at 76.71 ppm (peak s) due to ionic (or weakly ion paired) F_6acac, and $\delta(^1H)$ for the methine proton is 6.02 (peak h). The pyridine α protons in the 4:1 adduct are quite deshielded and appear as a doublet (J = 5 Hz) at 9.82 ppm (peak a). In $[(4\text{-}Cl(py))_4Pd](F_6acac)_2$, the pyridine ligands are twisted so that the aromatic rings are nearly perpendicular to the PdN_4 coordination plane. In this arrangement the α protons are located near the axial positions of palladium and are deshielded on account of the total magnetic anisotropy associated with the tetragonal d^8 system.[7]

The broad pyridine α-proton resonance at 8.9 ppm (peak b) is assigned to a 2:1 adduct that must surely be present as an intermediate, but no unique ^{19}F resonance is assigned to it. The ionic F_6acac in 2:1, 3:1 (if present), and 4:1 complexes undergo rapid exchange, which precludes detection of the individual peaks. For example, we note that the coordinated and ionic F_6acac groups in structurally characterized 2:1 complexes such as $[Pd(F_6acac\text{-}O,O')(bpy)]F_6acac$ and 3:1 complexes, e.g. $[Pd(F_6acac\text{-}O)(triphos)]F_6acac$, undergo rapid exchange so that, at room temperature, only averaged F_6acac resonances are seen.

With the more basic donor isopropylamine, $Pd(F_6acac\text{-}O,O')(F_6acac\text{-}C)\text{-}i\text{-}PrNH_2$ was detected when the amine:Pd ratio was 0.9:1; cf. Table II. As this ratio increased, a new, sharp ^{19}F peak at 75.03 ppm grew in intensity, and then decreased as amine:Pd exceeded 2:1. It was gradually replaced by another singlet at 77.65 ppm due to $[Pd(i\text{-}PrNH_2)_4](F_6acac)_2$. Assignment of the 75.03 ppm peak to $Pd(F_6acac\text{-}O,O')(F_6acac\text{-}O)\text{-}i\text{-}PrNH_2$ is based on the overall stoichiometry. If the 75.03 ppm peak is assigned to $(i\text{-}PrNH_2)_2Pd(F_6acac)_2$ and the 77.65 ppm peak to $[Pd(i\text{-}PrNH_2)_4](F_6acac)_2$, then insufficient $i\text{-}PrNH_2$ is available to account for the F_6acac peak ratios. Thus, the 75.03 ppm peak was assigned to a Pd species with only one $i\text{-}PrNH_2$. The F_6acac peak at 77.65 is assigned to both the L_2 and L_4 species that, as in the pyridine case, undergo rapid F_6acac exchange.

The $Pd(F_6acac)_2L_2$:$Pd(F_6acac)_2L_4$ ratio was determined by requiring that the $i\text{-}PrNH_2$:F_6acac ratio from the proton spectrum account for all the F_6acac species observed in the fluorine spectrum. This ratio is thus subject to considerable error when the $L_2Pd + L_4Pd$ levels are low.

p-Dithiane (1,4-dithiacyclohexane) reacts with $Pd(F_6acac)_2$ to form $[Pd(C_4H_8S_2)_2](F_6acac)_2$ as the sole isolated product. Vibrational, X-ray photoelectron, and NMR spectroscopic data suggested that, in this material, the cyclic ligand adopts a boat conformation, allowing both sulfur atoms to bind to the palladium. The dithiane adduct is therefore a member of the 4:1 ligand:palladium class of adducts.[6] When the p-dithiane:$Pd(F_6acac)_2$ ratio was 0.5:1 in 4:1 $CD_3CN\text{-}CDCl_3$, ^{19}F NMR spectra showed two singlets in a 1:1 ratio at 74.44 and 76.64 ppm, which are attributed to $Pd(F_6acac\text{-}O,O')(F_6acac\text{-}C)(\eta^1\text{-}C_4H_8S_2)$. This compound had nonequivalent methine protons with δ 5.08 and 6.13, and the spectroscopic assignment was confirmed by observation of a strong infrared band at 1735 cm^{-1} due to the F_6acac-C group. A broad ^{19}F resonance at ca. 75.7 ppm due to $[Pd(C_4H_8S_2)_2](F_6acac)_2$ sharpened, grew in intensity, and shifted to 76.3 ppm as increasing amounts of dithiane were added.

The F_6acac:dithiane ratios at low dithiane levels show multiple coordination of the dithiane to the Pd. Thus at 0.5:1 dithiane:$Pd(F_6acac)_2$, the unreacted $Pd(F_6acac)_2$ level is 34% and the $Pd(F_6acac\text{-}O,O')(F_6acac\text{-}C)(\eta^1\text{-}C_4H_8S_2)$ level is 18%. A broad peak at 75.73 ppm may be attributed to exchanging F_6acac in $Pd(F_6acac)_2(C_4H_8S_2)Pd(F_6acac)_2$ and $Pd(F_6acac)_2(C_4H_8S_2)$.

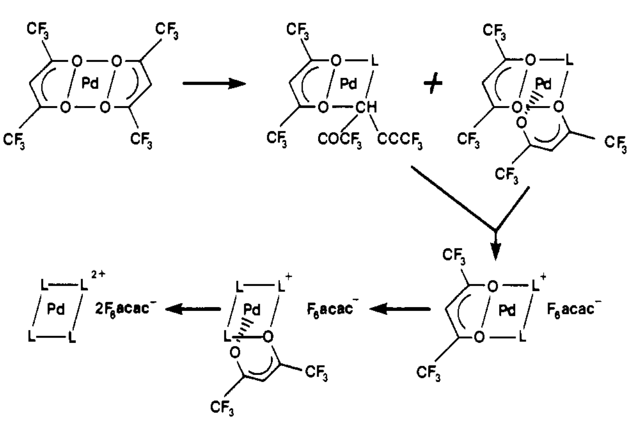

Figure 4. Sequential nucleophilic displacement reactions of $Pd(F_6acac)_2$.

Excess triphenylarsine and $Pd(F_6acac)_2$ form only the 2:1 adduct $[Pd(F_6acac\text{-}O,O')(Ph_3As)_2]F_6acac$. However, when the arsine:Pd ratio is less than 1:1, $Pd(F_6acac\text{-}O,O')(F_6acac\text{-}C)Ph_3As$ is observed. As more triphenylarsine is added, peaks in the ^1H and ^{19}F NMR spectra at 5.91 and 75.97 ppm, respectively, due to exchanging F_6acac in the 2:1 complexes, grew in intensity. The ratios of the 1:1 and 2:1 complexes were calculated by using the total ligand:$F_6(acac)_2$ stoichiometry found in the proton spectrum after correcting for the contribution from $Pd(F_6acac\text{-}O,O')(F_6acac\text{-}C)Ph_3As$.

tert-Butyl isocyanide forms discrete 2:1 and 4:1 complexes with $Pd(F_6acac)_2$, but the NMR spectra are greatly complicated by dissociation of the isocyanide ligands in solution. Indeed, the 4:1 complex can be converted to the 2:1 analogue simply by recrystallization from hexane. However, at isocyanide:Pd ratios of ~1:1, $Pd(F_6acac\text{-}O,O')(F_6acac\text{-}C)\text{-}t\text{-}C_4H_9NC$ was the major species in solution.

Discussion

The reactions of $Pd(F_6acac)_2$ with molecular Lewis bases involve sequential cleavage of the four Pd–O bonds between the metal and the two bidentate F_6acac groups. The result of these successive displacements is the generation of the adducts $Pd(F_6acac)_2L_n$ (n = 1–4). This chemistry is summarized in Figure 4, in which an exemplary member of each adduct type has been fully characterized by ^{19}F DNMR and X-ray crystallography. It is, in many respects, similar to the schematic sequence developed by Kawaguchi and co-workers.[16] As noted before,[4-8] the composition of *isolated* crystalline complexes depends on the steric and electronic properties of the base. In solution, competing and successive reactions are observed, and the situation is more complex.

In the initial nucleophilic attack on $Pd(F_6acac)_2$, formation of a ligand–Pd bond is accompanied by rearrangement of one of the bidentate, F_6acac-O,O' ligands to a monodentate, carbon-bonded F_6acac-C isomer. A parallel reaction, not involving F_6acac rearrangement, produces $Pd(F_6acac\text{-}O,O')(F_6acac\text{-}O)\cdot L$. The former isomer predominates when the ligand is pyridine or triphenylarsine, and none of the latter isomer is detected by NMR when the ligand is 1,4-dithiacyclohexane or *tert*-butyl isocyanide.

The displacement sequence stops at the 1:1 adduct state when the ligand is sterically hindered or contains large bulky groups; examples of such donors include phenazine, phen-

---

(16) S. Okeya, H. Sazaki, M. Ogita, T. Takemoto, Y. Onuki, Y. Nakemura, B. K. Mahapatra, and S. Kawaguchi, *Bull. Chem. Soc. Jpn.*, **54**, 1978 (1981).

oxathiin, and 2,6-dimethylpyridine. Less hindered bases attack both Pd(F$_6$acac-*O*,*O*′)(F$_6$acac-*O*)·L and Pd(F$_6$acac-*O*,*O*′)(F$_6$acac-*C*)·L, evidently at comparable rates, to form members of the 2:1 adduct class, [Pd(F$_6$acac-*O*,*O*′)L$_2$]F$_6$acac. ^{19}F DNMR spectroscopy has shown that, in these compounds, there is a rapid exchange between ionic and F$_6$acac-*O*,*O*′ so that they display only a broad singlet ^{19}F resonance at room temperature.[5] The reaction of Pd(F$_6$acac)$_2$ with silica and alumina appears, on the basis of vibrational and electronic spectroscopy, to produce similar 2:1 adducts in which surface oxide or hydroxyl groups serve as donor sites.[9,10] This class of adduct may be favored on oxide surfaces because of the decrease in entropy associated with the formation of a O–M–O–M–O–Pd(F$_6$acac)$^+$ ring. In all of the Pd(F$_6$acac)$_2$ complexes studied so far, the metal has a square-planar coordination core with four short Pd–O or Pd–ligand bonds, reflecting the preference of palladium for a 16-electron configuration. Displacement of the remaining F$_6$acac-*O*,*O*′ ligand by surface donor sites on silica or alumina appears improbable since examination of molecular models indicates that it is not possible to attach a palladium atom to a MO$_4$ or MO$_6$ unit (M = Si, Al) so that Pd and three or more oxygen atoms will be coplanar and will be within bonding distance, ca. 2.1 Å. In the surface adducts, the F$_6$acac-*O*,*O*′–F$_6$acac$^-$ exchange process provides an additional mechanism for reduction of the ^{19}F spin–lattice relaxation time, which was not considered in our earlier NMR experiments with Pd(F$_6$acac)$_2$ adsorbed on colloidal silica.[10]

With the molecular donors 2,2′-bipyridyl, phenanthroline, triphenylarsine, phenothiazine, and phenoselenazine, nucleophilic attack at palladium in their 2:1 complexes is not observed. However, cleavage of the remaining Pd–O bonds in [Pd(F$_6$acac-*O*,*O*′)L$_2$]$^+$ by smaller and/or stronger bases such as NH$_3$, MeNH$_2$, pyridine, and imidazole proceeds readily. According to Figure 4, the next step in the displacement sequence is [Pd(F$_6$acac-*O*)L$_3$]$^+$. In this $n = 3$ class of complexes, the planar, monodentate oxygen-bonded F$_6$acac is twisted so that it is nearly perpendicular to the palladium coordination plane. In this geometry, the other oxygen terminus lies in an axial position about 2.7 Å from the metal, which has a greatly distorted square-pyramidal coordination core. Crystalline members of this class have been isolated only when chelating, tridentate ligands such as triphos ((1,2-bis(diphenylphosphino)ethyl)phenylphosphine) and 2,2′,2″-terpyridyl are used. We consider that the intermediacy of 3:1 adducts containing monodentate donors is putative but quite reasonable in view of the isolation of analogues containing tridentate donors.

Nucleophilic cleavage of the last short Pd–O bond finally produces [PdL$_4$](F$_6$acac)$_2$. Such 4:1 adducts have been observed where the ligand is a relatively unhindered base such as NH$_3$, CH$_3$NH$_2$, (CH$_3$)$_2$NH, Ph$_3$Sb, *t*-C$_4$H$_9$NC, and pyridine and chelating ligands such as Ph$_2$E(CH$_2$)$_n$EPh$_2$ (E = P, As; n = 1, 2). Compounds having a 5:1 ligand:Pd ratio, resulting from further nucleophilic attack, have not been observed in our ^{19}F NMR experiments, but salts of Pd[Pd(OR)$_3$]$_5$$^{2+}$ have been characterized by ^{31}P DNMR.[17]

Displacement reactions effected by monodentate phosphines are rather different from those involving nitrogen and sulfur donors. This is particularly apparent in the chemistry of (aryl)$_3$P, which generates, fluxional Pd(F$_6$acac-*O*,*O*′)(F$_6$acac-*O*)P(aryl)$_3$ in high yield.[8,18,19]

Further reaction with (aryl)$_3$P proceeds only in ionizing solvents such as methanol and forms [(aryl)$_3$P]$_2$Pd(F$_6$acac-*O*,*O*′)$^+$. The displacement reactions affected by phosphines are analogous in some respects to those elucidated by Fackler and co-workers for metal 1,1-dithiolate complexes of nickel, palladium, and platinum. The five-coordinate M(S–S)$_2$PR$_3$ (S–S = 1,1-dithiolate ligand) compound is isolable when M is nickel. The palladium and platinum compounds feature planar, four-coordinate MPS$_3$ coordination geometries with a dangling, monodentate dithiolate ligand. In addition, ionic products of the type [M(S–S)(PR$_3$)$_2$]$^+$(S–S)$^-$ are formed.[20,21] The hexafluoroacetylacetonate analogues of Pt(acac-*O*)$_2$(PEt$_3$)$_2$[18,19] appear not to be produced by Pd(F$_6$acac)$_2$.

In conclusion, the scope of the acid–base chemistry of Pd(F$_6$acac)$_2$ derives from the strong acceptor character of the metal center and the relative weakness of the four Pd–O bonds. Successive rupture of these bonds and displacement of the F$_6$acac ligands lead to the production of the Pd(F$_6$acac)$_2$L$_n$ (n = 1–4) adducts.

Experimental Section

Palladium bis(hexafluoroacetylacetonate) was synthesized from aqueous NaF$_6$acac and Na$_2$PdCl$_4$ and purified by recrystallization from hexane followed by vacuum sublimation.[5] The melting point and heat of fusion, determined by differential scanning calorimetry, are 99.6 °C and 5.30 kcal/mol. X-ray powder pattern [d, Å (I/I_0)]: 8.91 (100), 2.77 (40), 3.05 (60), 6.06 (33). Electronic spectrum (cyclohexane): $\lambda_{\max}$ at 340 (sh) and 356 nm (log ϵ = 3.86). Beer's law is followed. Cyclic voltammograms showed irreversible reduction waves at −0.71 and −1.13 V in CH$_2$Cl$_2$ and at −0.15 V in CH$_3$CN (0.1 M Bu$_4$NClO$_4$; Pt electrode vs. SCE). ^{13}C NMR (CH$_2$Cl$_2$): δ 176.6 (CO, J_{CF} = 38 Hz), 115.2 (CF$_3$, J_{CF} = 283 Hz), 94.4 (CH, J_{CH} = 170 Hz). IR (Nujol): 3140 (w), 1600 (s), 1560 (m), 1450 (s), 1345 (m), 1265 (s), 1230 (s), 1210 (s), 1175 (s), 1155 (s), 1105 (s), 810 (s), 750 (m), 715 (m), 600 (m) cm^{-1}. The solubility in organic solvents is quite high, 35 g/L in hexane at 23 °C.

^{1}H and ^{19}F NMR spectra were obtained on a Varian XL-100 spectrometer. Chemical shifts are expressed relative to internal (CH$_3$)$_4$Si or CFCl$_3$. The organic ligands used in this work were of good commercial quality and were not purified further except for triphenylarsine, which was recrystallized from ethanol. Solution infrared spectra were obtained on a Nicolet 7199 Fourier transform interferometer. Peak positions are believed to be accurate to within ±1 cm^{-1}.

A small quantity of Pd(F$_6$acac)$_2$ was sealed under vacuum in a glass tube. This was kept overnight in a 50 °C oven, during which time needle crystals of the compound grew from the walls of the tube. These were removed and used for the X-ray diffraction experiments.

Collection and Reduction of X-ray Data. A summary of crystal data is presented in Table V. A crystal of Pd(F$_6$acac)$_2$ of dimensions 0.30 × 0.15 × 0.10 mm was sealed in a capillary tube to prevent sublimation. The crystal was found to belong to the triclinic crystal class by the Enraf-Nonius CAD 4-SDP peak search, centering, and indexing programs.[22] The space group $P\bar{1}$ was chosen and was verified by successful solution and refinement (vide infra). Data collection was carried out on a CAD 4 Nonius diffractometer. Background counts were measured at both ends of the scan range with the use of an ω–2θ scan, equal, at each side, to one-fourth of the scan range of the peak. In this manner, the total duration of background measurements is equal to half of the time required for the peak scan. The intensities of three standard reflections were measured every 1.5 h of X-ray exposure, and no decay with time was noted. The data were corrected for Lorentz, polarization, and background effects. An absorption correction was not applied since ψ scans on several reflections showed such a correction to be unnecessary.

---

(17) P. Meakin and J. P. Jesson, *J. Am. Chem. Soc.*, **96**, 5751 (1974).

(18) T. Ito, T. Kiriyama, and A. Yamamoto, *Chem. Lett.*, 835 (1976).

(19) S. Okeya, Y. Nakamura, and S. Kawaguchi, *Bull. Chem. Soc. Jpn.*, **54**, 3396 (1981).

(20) J. P. Fackler, Jr., L. D. Thompson, I. J. B. Lin, T. A. Stephenson, R. O. Gould, J. M. C. Alison, and A. J. F. Fraser, *Inorg. Chem.*, **21**, 2397 (1982).

(21) J. P. Fackler, Jr., and W. H. Pan, *J. Am. Chem. Soc.*, **101**, 1607 (1979).

(22) All calculations were carried out on PDP8A and 11/34 computers with use of the Enraf-Nonius CAD 4-SDP programs. This crystallographic computing package is described by B. A. Frenz in "Computing in Crystallography", H. Schenk, R. Olthof-Hazekamp, H. van Koningsveld, G. C. Bassi, Eds., Delft University Press, Delft, Holland, 1978, pp 64–71, and "CAD 4 and SDP User's Manual", Enraf-Nonius, Delft, Holland, 1978.

Table V. Summary of Crystal Data and Intensity Collection

Crystal Parameters	
cryst syst, space group	triclinic, $P\bar{1}$
a, Å	12.279 (4)
b, Å	12.815 (2)
c, Å	4.894 (2)
α, deg	93.63 (2)
β, deg	91.81 (3)
γ, deg	89.51 (2)
V, Å^3	768.1 (7)
Z	2
calcd density, g/cm^3	2.250
temp, °C	23
abs coeff, cm^{-1}	13.6
formula	$C_{10}H_2F_{12}O_4Pd_1$
fw	520.5
Measurement of Intensity Data	
diffractometer	CAD4
radiation	Mo Kα (λ = 0.710 69 Å), graphite monochromatized
scan range, 2θ, deg	0–50
unique reflectns measd	333.4 ($+h,\pm k,\pm l$)
no. of obsd reflectns^a	2073 [$F_o^2 \geqslant 2.0(F_o^2)$]
refinement	full-matrix least squares
no. of parameters	248
R^b	0.063
$R_w{}^b$	0.084
GOF	3.3
p^b	0.03

[a] The intensity data were processed as described in "CAD4 and SDP User's Manual", Enraf-Nonius, Delft, Holland, 1978. The net intensity I is given as $I = [K/(\mathrm{NPI})](C - 2B)$, where $K = 20.166 \times$ attenuator reactor, NPI = ratio of fastest possible scan rate to scan rate for measurement, C = total count, and B = total background count. The standard deviation in the net intensity is given by $[\sigma(I)]^2 = (K/\mathrm{NPI})^2[C + 4B + (pI)^2]$, where p is a factor used to downweight intense reflections. The observed structure factor amplitude F_o is given by $F_o = (I/Lp)^{1/2}$; where Lp = Lorentz and polarization factors. The $\sigma(I)$'s were converted to the estimated errors in the relative structure factors $\sigma(F_o)$ by $\sigma(F_o) = {}^1/_2(\sigma(I)/I)F_o$. [b] The function minimized was $\Sigma w(|F_c| - |F_o|)^2$, where $w = 1/[\sigma(F_o)]^2$. The unweighted and weighted residuals are defined as $R = (\Sigma ||F_o| - |F_c||)/\Sigma |F_o|$ and $R_w = [(\Sigma w(|F_o| - |F_c|))^2/(\Sigma w|F_o|)^2]^{1/2}$. The error in an observation of unit weight (GOF) is $[\Sigma w|F_o| - |F_c|^2/(\mathrm{NO} - \mathrm{NV})]^{1/2}$, where NO and NV are the number of observations and variables, respectively.

Solution and Refinement of the Structure. The structure was solved by conventional heavy-atom techniques. Pd atoms were placed on the special positions 0, 0, 0 and $^1/_2$, $^1/_2$, $^1/_2$ so that each molecule is centric. Difference-Fourier calculations were used to locate all remaining non-hydrogen atoms. The atomic scattering factors were taken from the usual tabulation,[23] and the effects of anomalous dispersion were included in F_c by using Cromer and Ibers'[24] values of $\Delta f'$ and $\Delta f''$. A table of observed and calculated structure factor amplitudes is available.[25] The two hydrogen atom positions were calculated and included in the structure factor calculations but were not refined. All non-hydrogen atoms were refined by using anisotropic thermal parameters. The final difference-Fourier map did not reveal any chemically significant features. The largest peaks in this map were 0.5 e/Å and were located near the fluorine atoms. Some disorder was evident in the fluorine positions; however, the residual electron density in the final difference-Fourier map did not suggest an obvious disorder model. Therefore, this point was not pursued. The final positional and thermal parameters of the atoms appear in Table I. The labeling scheme is shown in Figure 1.

Acknowledgment. The authors are grateful to members of the 3M Analytical and Properties Research Laboratory for the physical measurements on Pd(F_6acac)$_2$ and its derivatives and to Professors J. P. Fackler, Jr., and Shinichi Kawaguchi for preprints of their work. The National Science Foundation is acknowledged for partial support of the X-ray diffraction and structure-solving equipment at the University of Minnesota (Grant CHE77-28505). L.H.P. also acknowledges support by the National Science Foundation (Grant CHE-8108490) of his contribution to this paper.

Registry No. Pd(F_6acac)$_2$, 64916-48-9; Pd(F_6acac-*O*,*O'*)(F_6acac-*C*)py, 85976-96-1; Pd(F_6acac-*O*,*O'*)(F_6acac-*O*)py, 85976-97-2; [Pd(F_6acac-*O*,*O'*)(py)$_2$]F_6acac, 85976-99-4; [Pd(py)$_4$](F_6acac)$_2$, 65353-63-1; Pd(F_6acac-*O*,*O'*)(F_6acac-*C*)Ph_3As, 85977-00-0; Pd(F_6acac-*O*,*O'*)(F_6acac-*O*)Ph_3As, 85977-01-1; [Pd(F_6acac-*O*,*O'*)(Ph_3As)$_2$]F_6acac, 78128-23-1; Pd(F_6acac-*O*,*O'*)(F_6acac-*C*)(*i*-$PrNH_2$), 85977-02-2; Pd(F_6acac-*O*,*O'*)(F_6acac-*O*)(*i*-$PrNH_2$), 85977-03-3; [Pd(F_6acac-*O*,*O'*)(*i*-$PrNH_2$)$_2$]F_6acac, 85977-05-5; [Pd(*i*-$PrNH_2$)$_4$](F_6acac)$_2$, 85977-07-7; Pd(F_6acac-*O*,*O'*)(F_6acac-*C*)(η^1-$C_4H_8S_2$), 85977-08-8; Pd(F_6acac-*O*,*O'*)(F_6acac-*O*)(η^1-$C_4H_8S_2$), 85977-09-9; Pd(F_6acac-*O*,*O'*)(F_6acac-*C*)(*t*-C_4H_9NC), 85977-10-2; Pd(F_6acac-*O*,*O'*)(F_6acac-*O*)(*t*-C_4H_9NC), 85995-10-4.

Supplementary Material Available: Tables S-1–S-3 showing observed and calculated structure factor amplitudes for Pd(F_6acac)$_2$, weighted least-squares planes, and anisotropic thermal parameters and their standard deviations (11 pages). Ordering information is given on any current masthead page.

---

(23) D. T. Cromer and J. T. Waber, "International Tables for X-ray Crystallography", Vol. IV, Kynoch Press, Birmingham, England, 1974, Table 2.2.4; D. T. Cromer, *ibid.*, Table 2.3.1.

(24) D. T. Cromer and J. A. Ibers in ref 23.

(25) See paragraph at end of paper regarding supplementary material.

Contribution from the Department of Chemistry,
City College of The City University of New York, New York, New York 10031

Kinetics and Mechanism of the Cerium(IV) Oxidation of Methylmalonic Acid and of Ethylmalonic Acid in Acid Media

FRANCES TISCHLER and JACK I. MORROW*

Received November 9, 1982

The kinetics and mechanism of the oxidation of methylmalonic acid and of ethylmalonic acid by cerium(IV) in acid media was studied with use of the stopped-flow technique. The observed rate law was found to be of the form $-d[\mathrm{Ce(IV)}]/dt = k_H[\mathrm{Ce(IV)}][\mathrm{RCH(CO_2H)_2}]$. The second-order rate constant, k_H, was found to be hydrogen ion dependent and of the form $k_H = (k[\mathrm{H^+}]^2 + k'[\mathrm{H^+}] + k'')/([\mathrm{H^+}] + K)$. A mechanism consistent with these results is proposed.

Introduction

The role played by the hydrogen ion in the oxidation of organic and inorganic substrates by metal ions sheds considerable light on the mechanism of these reactions and the possibility of intermediate complex formation. Some reactions are acid catalyzed such as in the Ce(IV) oxidation of various alcohols[1-3] and carboxylic acids[4,5] while others such as the

---

(1) M. Ardon, *J. Chem. Soc.*, 1811 (1957).

(2) M. Rangaswamy and M. Santappa, *Indian J. Chem.*, 7, 473 (1969).

0020-1669/83/1322-2286$01.50/0 © 1983 American Chemical Society